Semiconductor Physics, Quantum Electronics & Optoelectronics. 2003. V. 6, N 1. P. 97-101.

PACS: 07.07.Df, 77.65.Ly, 85.30.Kk

About manifestation of the piezojunction effect in diode temperature sensors

V.L. Borblik,Yu.M. Shwarts, E.F. Venger

Institute of Semiconductor Physics, NA Sciences of Ukraine, 45 prospect Nauky, 03028 Kyiv, Ukraine
Phone: +38(044) 265 6292, e-mail: borblik@lab2.semicond.kiev.ua

Abstract. An analytical theory of piezojunction effect has developed in application to silicon diode temperature n^+-p type sensors, which for the first time takes into account three-subbands structure of the valence band of silicon. The compressive and tensile stresses (along the main crystallographic directions), long- and short-base diodes, longitudinal and transverse effects have been considered.

It is shown that the three-subbands model results in even more nonlinear dependence of changes in the sensor readings on stress value (in comparison with the two-subbands model), holds minimality of the longitudinal piezojunction effect under stress orientation along the [100] direction and predicts substantially larger effect value for the strain perpendicular to the current through the diode.

Keywords: diode temperature sensor, mechanical stress, piezojunction effect, silicon.

Paper received 27.12.02; accepted for publication 18.03.03.

1. Introduction

Up-to-date semiconductor diodes and transistors which are used as temperature sensors, are of small enough sizes (of the order of tens micrometers) and it is possible that internal mechanical stresses appear in them (under manufacturing and subsequent exploitation) capable to influence on operation of these devices. This influence is of complex nature because is accompanied by changes in properties of both n- and p- region of the diode.

A few attempts of analytical calculation of the piezojunction effect are known (under a number of serious simplifications). So, in Ref. 1 light and heavy holes were not distinguished and the changes in carrier mobilities with deformation were ignored, and in Ref. 2 a limit of large strains was used which was not adequate to moderate mechanical stresses (≤ 200 MPa) appearing in the device structures.

Recently, the numerical methods have become to be used [3, 4] capable to take into account all details of semiconductor band structure under stress. But this approach is very laborious and requires huge computer resources. Herewith, in spite of a sufficiently large number of specific cases calculated, conditions for piezojunction effect minimization were not brought to light up to now.

In our previous paper [5], it was shown that silicon n^+-p diodes under moderate mechanical stresses can be considered by analytical methods because in this case mobility of minority carriers (electrons) is calculated easily in the framework of electron transfer mechanism [6], and, as for holes, it is enough to know splitting values (and shifts) for degenerate edge of the valence band; the so-called carrier concentration effective mass for the valence band of Si does not change practically under these conditions [7].

As a result of this consideration, it was shown in Ref. 5 that, at parallel orientations of the diode current and mechanical stress, the piezojunction effect in silicon n^+-p diodes is minimal in the direction of [100]-axis (when piezoresistance of n-Si is maximal) rather than in the [111] direction when it is minimal. Apparent paradoxality of this result is connected with the fact that it is the [100] direction in which substantial changes in the electron mobility are compensated by about the same changes in the intrinsic carrier concentration; therefore, two components of the effect cancel each other to a high degree.

The changes in energy spectrum of holes under mechanical stress were considered in Ref. 5 on the basis of Bir-Pikus' theory [8] which did not take into account interaction of light and heavy holes with spin-orbit split-off hole subband. In Si spin-orbit splitting of the valence band is known to be small enough (~ 0.044 eV) and above interaction can give noticeable effect [9].

In this paper, an analytical theory of the piezojunction effect in silicon n^+-p-type diode temperature sensors is developed taking into consideration the interaction and contribution into conductivity of all three subbands of the valence band. Herewith, along with the longitudinal effects, the transverse effects are considered as well, when the diode current and uniaxial strain are orthogonal to each other.

2. Starting relations

Junction diodes (or emitter-base junctions of transistors), when they are used as the temperature sensors, operate in a given current regime. If diffusion of injected minority carriers in the device base dominates, its piezoresistance is caused by the effect of mechanical stress $\hat{\sigma}$ on the device saturation current that results in change, ΔU, in a voltage drop across the junction

$$\Delta U(\hat{\sigma}) = -\frac{kT}{q}\ln\left(\frac{J_s(\hat{\sigma})}{J_s(0)}\right) \tag{1}$$

where q is elementary charge, k is the Boltzmann's constant, T is temperature, J_s is the saturation current density that is given by the expression (see, for example, [1])

$$J_s = kT\frac{n_i^2}{N_B}\frac{\mu_n}{L_n}\operatorname{cth}\left(\frac{d}{L_n}\right). \tag{2}$$

In Eq. (2) n_i is the intrinsic carrier concentration, N_B is the base doping level (for simplicity, the step-like doping profile is supposed), μ_n and L_n are mobility and diffusion length of the minority carriers (electrons), d is the base length. Here and hereinafter the classic statistics is assumed to be applicable.

In the diodes with long base ($d >> L_n$, just for them the theory in Ref. 2 was developed) Eq. (1) takes the form

$$\Delta U(\hat{\sigma}) = -\frac{kT}{q}\ln\left[\frac{n_i^2(\hat{\sigma})}{n_i^2(0)}\left(\frac{\mu_n(\hat{\sigma})}{\mu_n(0)}\right)^{1/2}\right] \tag{3}$$

where the minority carrier lifetime, τ_n, is considered to not vary with the strain. But in the diodes with short base (or in transistors, just for them calculations in Ref. 3,4 were carried out) when $d << L_n$, Eq. (1) is reduced to some other expression

$$\Delta U(\hat{\sigma}) = -\frac{kT}{q}\ln\left[\frac{n_i^2(\hat{\sigma})}{n_i^2(0)}\frac{\mu_n(\hat{\sigma})}{\mu_n(0)}\right]. \tag{4}$$

As it follows from Eqs (3) and (4), effect of mechanical stress on the temperature sensor readings occurs at the expense of changes in both the carrier mobility (analog of piezoresistance in a case of semiconductor resistor) and the intrinsic carrier concentration (additional, solely diode effect). Both effects are consequences of the changes in semiconductor energy spectrum under stress.

3. Changes in the energy spectrum of electrons and holes in silicon under stress

Change in the energy spectrum of electrons in Si under uniaxial elastic strain (of moderate magnitude) is reduced, mainly, to the shift, $\delta E_c = E_c - E_{c0}$, of equivalent valleys in energy [6]:

$$\delta E_c^{(m)} = \sum_{ij}\left[\Xi_d\delta_{ij} + \Xi_u e_i^{(m)} e_j^{(m)}\right]u_{ij} \tag{5}$$

where superscript m is the valley number, $\vec{e}^{\,(m)}$ is the unit vector directed to the center of mth valley from the origin of coordinates in the reciprocal crystal lattice, u_{ij} is the strain tensor, Ξ_d and Ξ_u are the deformation potentials of the conduction band.

If the strain is such that different valleys shift differently, then electron transfer effect takes place, which is the main cause of electron mobility changes. The change in their mobility (if they are considered like majority carriers) occurs in accordance with the expression

$$\mu_n(\hat{\sigma}) = \sum_{m=1}^{3}\frac{n^{(m)}(\hat{\sigma})}{n(0)}\mu_n^{(m)}, \tag{6}$$

where $n^{(m)}(\hat{\sigma})$ is the population of a pair of the valleys located on the axis of <100>–type, $\mu_n^{(m)}$ is the electron mobility along the current direction in each of 3 pairs of these valleys, $n(0)$ is the total electron concentration.

Change in the energy spectrum of holes is reduced to lifting of the valence band degeneracy at the wave vector $\vec{k} = 0$ and deformation of dispersion law for all kinds of holes. Taking into account interaction of two lower subbands with split-off hole subband, the shifts, $\delta E_v^{h,l,s-o} = E_v^{h,l,s-o} - E_{v0}^{h,l,s-o}$, of the subband edges for heavy (h), light (l), and split-off (s-o) holes are given, in accordance with Ref. 9 , by

$$\begin{aligned}
\delta E_v^h &= a(u_{xx}+u_{yy}+u_{zz})+\varepsilon,\\
\delta E_v^l &= a(u_{xx}+u_{yy}+u_{zz})-\\
&-\left(\varepsilon+\Delta_{s-o}-\sqrt{9\varepsilon^2+\Delta_{s-o}^2-2\varepsilon\Delta_{s-o}}\right)\Big/2,\\
\delta E_v^{s-o} &= a(u_{xx}+u_{yy}+u_{zz})-\\
&-\left(\varepsilon+\Delta_{s-o}+\sqrt{9\varepsilon^2+\Delta_{s-o}^2-2\varepsilon\Delta_{s-o}}\right)\Big/2,
\end{aligned} \tag{7}$$

where Δ_{s-o} is the energy of spin splitting of the valence band, $\varepsilon = -b(u_{zz}-u_{xx})$ under stress along [001] axis,

$\varepsilon = -\frac{d}{\sqrt{3}} u_{xy}$ under stress along [111] axis, a, b and d are the deformation potentials for the valence band.

For the stress, oriented along the third basic crystallographic direction ([110]), analytical solution of the problem is absent. However, at close values of ε for two previous stress orientations (that is approximately the situation for Si) splitting of the light and heavy hole subbands proves to be practically the same at any orientations of mechanical stress [9,10]. Below, in numerical calculations for stress oriented along [110]-axis, we use the same value of ε as for [100] direction.

The components u_{ij} of the strain sensor which enter in the Eqs (5) and (7) are expressed in the terms of the stress tensor σ_{kl} by means of Hooke's law

$$u_{ij} = \sum_{kl} S_{ijkl} \sigma_{kl} \ , \tag{8}$$

where S_{ijkl} are components of elastic compliance tensor of the 4th rank. When using of pair-wise subscripts (in accordance with the scheme $xx \to 1$, $yy \to 2$, $zz \to 3$, $yz \to 4$, $zx \to 5$, $xy \to 6$) the tensor S_{ijkl} is replaced by the matrix $S_{\alpha\beta}$ with dimensions 6×6

$$u_\alpha = \sum_{\beta=1}^{6} S_{\alpha\beta} \sigma_\beta , \tag{9}$$

in which, for the crystals of cubic symmetry, only 3 independent components remain: S_{11}, S_{12}, S_{44} [10].

Herewith the changes in hole mobility occurs at the expense of both the deformation of their dispersion law (that is accompanied by changes in hole effective masses) and changes in relative subband occupation.

As well as in Ref. 5, we make use of the fact that in spite of the changes under stress in partial effective masses of different kinds of holes, their concentration effective mass, m_{cc}, [11] in the stress range being not in excess of 10^9 dyn/cm^2 does not vary practically [7] (see Tab. 1). This situation allows us to take into account the effect of the hole subbands repopulating only keeping as invariable their effective masses. For comparison, however, under the stress oriented along the [100] direction, the changes in effective masses were taken into consideration as well (through the concentration effective mass m_{cc}).

Then following, as a whole, to the same calculation scheme as in Ref. 5, we obtain the expression for ratio $n_i^2(\hat{\sigma}) / n_i^2(0)$ in the form

$$\frac{n_i^2(\hat{\sigma})}{n_i^2(0)} = \frac{1}{3} \left[\frac{m_{h0}^{3/2} \exp\left(\delta E_v^h / kT\right) + m_{l0}^{3/2} \exp\left(\delta E_v^l / kT\right) + m_{s-o,0}^{3/2} \exp((\delta E_v^{s-o} - \Delta_{s-o}) / kT)}{m_{h0}^{3/2} + m_{l0}^{3/2} + m_{s-o,0}^{3/2} \exp(-\Delta_{s-o} / kT)} \right], \tag{10}$$

$$\sum_{m=1}^{3} \exp(-\delta E_c^{(m)} / kT)$$

where m_{h0} , m_{l0} and $m_{s-o,0}$ are effective masses of heavily, light and split-off holes, respectively, in the absence of the stress.

Table 1. Variation of the hole concentration effective mass m_{cc} in Si with compressive stress along the [100] direction (in accordance with [7]).

Compressive stress along the [100] axis (dyn/cm^2)	m_{cc}/m_{cc0}
0	1
10^7	0.9998
10^8	0.9976
10^9	0.9751

The explicit expressions for stress-dependent normalized electron mobility obtained in accordance with Eq. (6) for a number of mutual orientations of the diode excitation current and mechanical stress, are presented in Tab. 2.

4. Numerical results

The mobility anisotropy constant $K = \mu_\perp / \mu_{\text{II}}$ involved in above mentioned expressions depends, generally speaking, on dominant scattering mechanism and temperature. However, for the sake of simplicity, we put it here to be equal to ratio of transversal and longitudinal electron effective masses, i.e. $K = 0.98/0.19 \approx 5.16$. Values of the rest material parameters of silicon used in calculation are shown in Tab. 3.

Fig. 1 represents, for illustration, calculation results for position of all hole subbands edges versus uniaxial stress value under deformation along [100] axis. Full curves represent the results of three-subbands theory [9], dashed curves are for two-subbands theory [8]. It is seen that more rigorous theory [9] becomes to manifest itself starting from the stress of the order of 10^9 dyn/cm^2 and affects only one of lower subbands.

Shown in Fig. 2 are the dependencies of the ratio $n_i^2(\hat{\sigma}) / n_i^2(0)$ (at $T = 300$ K) on uniaxial stress for three deformation directions. The results obtained on the basis of Hasegawa's theory [9] are shown by solid lines. Dashed lines represent the results obtained in accordance with the Bir-Pikus' theory [8] (they are taken from the previous paper [5]). Comparison of these results shows that more general theory [9] results in more substantial nonlinearity of above dependencies in comparison with the simpler theory [8]. This feature manifests itself also in analogous dependencies of $\Delta U(\hat{\sigma})$ (as it will be seen below).The short dotted curve (for [100] direction in the

Table 2. The expressions for normalized electron mobility for three basic stress orientations in longitudinal (1st column) and transverse (2nd column) orientations.

Uniaxial stress direction	$\mu_n(\hat{\sigma})/\mu_n(0)$ (at the current parallel to strain)	$\mu_n(\hat{\sigma})/\mu_n(0)$ (at the current along [001] axis)	parameter β in formulae for mobility
[100]	$\frac{3}{2K+1}\frac{1+2Ke^{\beta\sigma}}{1+2e^{\beta\sigma}}$	$\frac{3}{2K+1}\frac{1+K+Ke^{-\beta\sigma}}{2+e^{-\beta\sigma}}$	$\frac{\Xi_u(S_{11}-S_{12})}{kT}$
[110]	$\frac{3}{2K+1}\frac{1+K+Ke^{\beta\sigma}}{2+e^{\beta\sigma}}$	$\frac{3}{2K+1}\frac{1+2Ke^{-\beta\sigma}}{1+2e^{-\beta\sigma}}$	$\frac{\Xi_u(S_{11}-S_{12})}{2kT}$
[111]	1	1	—

Table 3. Silicon parameters used in calculation ([12]).

Deformation potentials (eV)	Value
Ξ_d	1.1
Ξ_u	10.5
a	2.1
b	–2.33
d	–4.75
$\Xi_d + \frac{1}{3}\Xi_u - a$	2.5
Elastic compliances (10^{-12} cm^2/dyn)	Value
S_{11}	0.768
S_{12}	–0.214
S_{44}	1.26

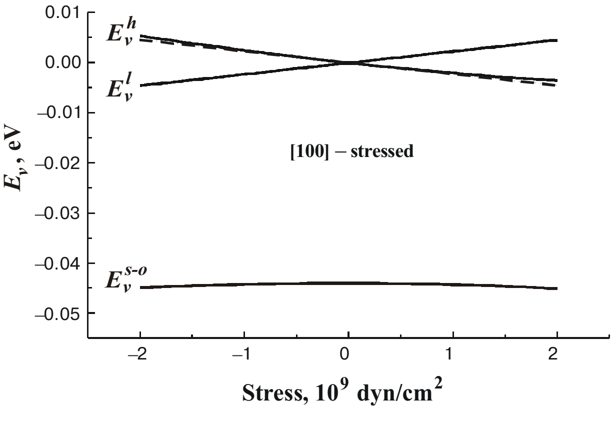

Fig. 1. Position of the subband edges in valence band of silicon versus uniaxial stress oriented along [100] axis; full lines are for Hasegawa's theory [9], dashed lines are for Bir-Pikus' one [8].

range of compressive stress from 0 to 10^9 dyn/cm^2) corresponds to exact result taking into account the changes in hole effective masses through the hole concentration effective mass m_{cc} according to [7].

Effect of the mechanical stress on electron mobility in Si (calculated on the basis of Tab. 2) is demonstrated by Fig. 3. It is seen from comparison of Fig. 2 and 3 that if

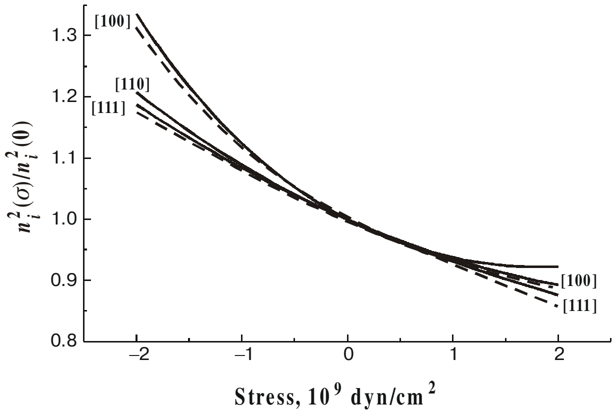

Fig. 2. Dependence of normalized square of the intrinsic carrier concentration on mechanical stress in three basic crystallographic directions; the solid curves is calculated under Hasegawa's theory, the dashed curves – under Bir-Pikus' one; short dotted curve corresponds to taking into account (for [100] direction) the change in the hole concentration effective mass.

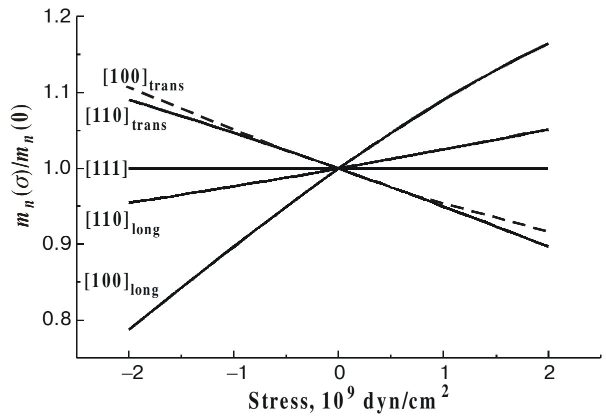

Fig. 3. Dependence of normalized electron mobility on mechanical stress in three basic crystallographic directions at longitudinal (long) and transverse (trans) orientations (in accordance with Tab. 2).

one proceeds from the case of [111]-oriented stress when longitudinal and transverse piezojunction effects are not differentiated (in considered approximation), then passing to other stress orientations is accompanied by the changes in mobility and intrinsic concentration in synchronism – at transverse piezoeffects, and by opposite changes in these quantities – at longitudinal ones. As a result, indications of the diode thermometer are changed the most strongly at the stress orientations transversal to the excitation current (see Fig. 4 for the long-base diode and Fig. 5 – for the short–base diode or transistor).

But at parallel orientation of the current and the stress there is a partial compensation of two components of the piezojunction effect, and its value decreases substantially. In particular, in the short–base diode this fact is especially pronounced: the $[100]_{\mathrm{long}}$ curve corresponding to the stress and the current along [100] is characterized by the least absolute value of $\Delta U(\hat{\sigma})$. The short dotted curves in Figs 4 and 5 correspond (as well as in Fig. 2) to exact calculations (for the stress along [100] axis) taking into account the changes in hole effective masses. In any case deviation of approximate results (which does not take into account changes of effective masses) from rigorous ones (including them through the effective mass m_{cc}) constitutes near one percent.

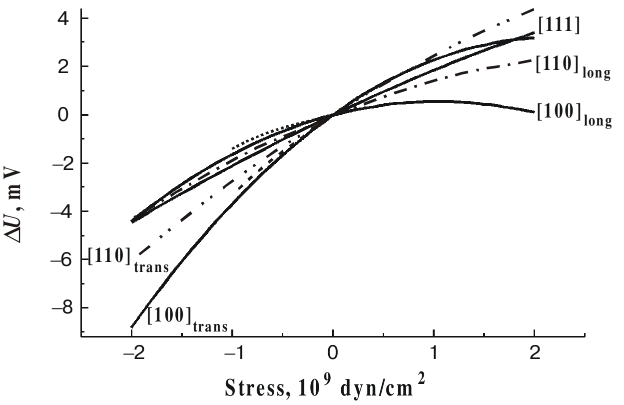

Fig. 4. Indication changes of the diode thermometer with long base versus mechanical stress; symbol 'long' means longitudinal orientation, symbol 'trans' – transversal one; the short dotted curves correspond to taking into account (for [100]-directed stress) the change in the hole concentration effective mass.

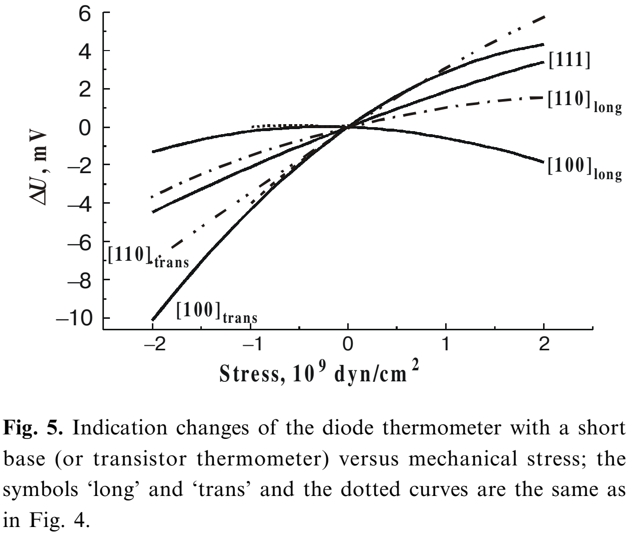

Fig. 5. Indication changes of the diode thermometer with a short base (or transistor thermometer) versus mechanical stress; the symbols 'long' and 'trans' and the dotted curves are the same as in Fig. 4.

Using for calculation other set of silicon parameters (in particular, from Ref. 13) qualitatively results in the same but yields some lower magnitudes of $\Delta U(\hat{\sigma})$.

5. Conclusion

So, in the framework of more rigorous (tree-subband) theory of *p*-Si, the minimal piezojunction effect in silicon n^+-*p* diodes also is the longitudinal one at the strain along [100] direction. But the transverse piezojunction effects prove to be substantially greater (if, of course, to be limited by the main crystallographic orientations, which are of the most practical interest only. It is obvious that rotation of the current direction in plane perpendicular to the stress or, on the contrary, rotation of the stress direction in plane perpendicular to the current, holds transverse character of the effect but can result in its smaller value in the intermediate orientations).

References

1. J.J. Wortman, J.R. Hauser and R.M. Burger, Effect of mechanical stress on p-n junction device characteristics // *J. Appl. Phys.* **35** (7), pp. 2122-2131 (1964).
2. Y.Kanda, Effect of stress on germanium and silicon p-n junction // *Jpn. J. Appl. Phys.* **6** (4), pp. 475-486 (1967).
3. J.F. Creemer and P.J. French, The piezojunction effect in bipolar transistors at moderate stress level: a theoretical and experimental study // *Sensors and Actuators* A82 (1-3), pp. 181-185 (2000).
4. J.F. Creemer, The effect of mechanical stress on bipolar transistor characteristics. Ph. D. Thesis of Delft University of Technology, 2002.
5. V.L. Borblik, Yu.M. Shwarts and E.F. Venger, Effect of mechanical stress on operation of diode temperature sensors // *Semicond. Physics, Quantum Electronics & Optoelectronics*, **5** (3), pp. 322-327 (2002).
6. C. Herring and E. Vogt, Transport and deformation-potential theory for many-valley semiconductors with anisotropic scattering // *Phys. Rev.* **101** (3), pp. 944-961 (1956).
7. T. Manku and A. Nathan, Valence-band structure for strained group-IV semiconductors // *J. Appl. Phys.* **73** (3), pp. 1205-1213 (1993).
8. G.L. Bir and G.E. Pikus, *Symmetry and stain-induced effects in semiconductors,* Wiley, New York ,1974.
9. H. Hasegawa, Theory of cyclotron resonance in strained silicon crystals // *Phys. Rev.* **129** (3), pp. 1029-1040 (1963).
10. J.C. Hensel and G. Feher, Cyclotron resonance experiments in uniaxially stressed silicon: valence band inverse mass parameters and deformation potentials // *Phys. Rev.* **129** (3), pp. 1041-1062 (1963).
11. F.L. Madarasz, J. E. Land and P.M. Hemeger, Effective masses for non-parabolic bands in p-type silicon // *J. Appl Phys.* **52** (7), pp. 4646-4648 (1981).
12. M.V. Fischetti and S.E. Laux, Band structure, deformation potentials and carrier mobility in strained Si, Ge, and SiGe alloys // *J. Appl. Phys.* **80** (4), pp. 2234-2252 (1996).
13. Friedel P., Hybertsen M. S. and Schluter M. Local empirical pseudopotential approach to the optical properties of Si/Ge superlattices // *Phys. Rev.* **B 39**, pp. 7974-7977 (1989).